Journal of Hazardous Materials 201–202 (2012) 250–259

Contents lists available at SciVerse ScienceDirect

Journal of Hazardous Materials

journal homepage: www.elsevier.com/locate/jhazmat

A graphene oxide-based electrochemical sensor for sensitive determination of 4-nitrophenol

Junhua Li[a,b,*], Daizhi Kuang[a,b], Yonglan Feng[a,b], Fuxing Zhang[a,b], Zhifeng Xu[a,b], Mengqin Liu[a,b]

[a] Department of Chemistry and Material Science, Hengyang Normal University, Hengyang, 421008, Hunan, PR China
[b] Key Laboratory of Functional Organometallic Materials of Hunan Province College, Hengyang Normal University, Hengyang, 421008, Hunan, PR China

ARTICLE INFO

Article history:
Received 5 September 2011
Received in revised form 7 November 2011
Accepted 23 November 2011
Available online 29 November 2011

Keywords:
Graphene oxide
Electrochemical sensor
4-Nitrophenol
Sensitive detection

ABSTRACT

A graphene oxide (GO) film coated glassy carbon electrode (GCE) was fabricated for sensitive determination of 4-nitrophenol (4-NP). The GO-based sensor was characterized by scanning electron microscope, atomic force microscopy and electrochemical impedance spectroscopy. The electrochemical behaviors of 4-NP at the GO-film coated GCE were investigated in detail. In 0.1 M acetate buffer with a pH of 4.8, 4-NP yields a very sensitive and well-defined reduction peak at the GO-modified GCE. It is found that the GO film exhibits obvious electrocatalytic activity toward the reduction of 4-NP since it not only increases the reduction peak current but also lowers the reduction overpotential. Based on this, an electrochemical method was proposed for the direct determination of 4-NP. Various kinetic parameters such as transfer electron number, transfer proton number and standard heterogeneous rate constant were calculated, and various experimental parameters were also optimized. Under the optimal conditions, the reduction peak current varies linearly with the concentration of 4-NP ranging from 0.1 to 120 μM, and the detection limit is 0.02 μM at the signal noise ratio of 3. Moreover, the fabricated sensor presented high selectivity and long-term stability. This electrochemical sensor was further applied to determine 4-NP in real water samples, and it showed great promise for simple, sensitive, and quantitative detection of 4-NP.

1. Introduction

The analysis of aromatic nitrocompounds such as nitrobenzene, nitrotoluenes and nitrophenols in natural waters and effluents is of prime importance for environmental control due to their appearance from a wide range of activities [1]. These compounds have toxic effect on humans, animals and plants and they give an undesirable taste and odor to drinking water, even at very low concentration [2]. For these reasons, many aromatic nitrocompounds have been included in the environmental legislation. In particular, 4-nitrophenol (4-NP) is one of the nitrophenols cited in the List of Priority Pollutants of the U.S.A. Environmental Protection Agency (EPA) due to its toxicity and persistence [3]. Acute inhalation or ingestion of 4-NP in a short time for humans can cause headaches, drowsiness, nausea and cyanosis [1]. In addition, 4-NP was reported as potential carcinogen, teratogens and mutagen [4], so its application should be strictly controlled and supervised. Unfortunately, 4-NP is still widely used as intermediates in the production of pharmaceuticals, dyestuffs and pesticides, such as fenitrothion and parathion insecticide which can reversely hydrolyze to form 4-NP [5,6]. In addition, 4-NP can also be used as leather fungicide and acid–base indicator [5]. Therefore, 4-NP will be inevitably released into environment to cause pollution during its production and application for agriculture and industry. Therefore, it is very urgent and important to develop simple and reliable method for determination of trace amounts of 4-NP in environment.

Until now, the widely used methods for determination of 4-NP are spectrophotometry [7], fluorescence [8], gas chromatography (GC) [9], capillary electrophoresis [4] and high performance liquid chromatography (HPLC) [10]. Traditional spectrophotometry and colorimetric methods are easily interfered by related compounds. GC methods can sometimes require relatively expensive reagents and need beneficiation and derivatization before analysis and it cannot be used directly to aqueous samples. HPLC and capillary electrophoresis methods are good alternative methods, but they need high cost to buy columns and waste more organic solvents [7]. Thus, there is a demand for new analytical technique with cheap instrument, low cost, simple operation, time saving and real-time detection for 4-NP. Moreover, the easy electrochemical reduction of nitro groups at the aromatic or heterocyclic ring, whose mechanism is discussed in monographs [11], permits very sensitive determinations of a number of genotoxic and ecotoxic nitro-compounds using modern voltammetric techniques at modified electrodes [12]. In this regard, electrochemically analytical technique is an

* Corresponding author at: Department of Chemistry and Material Science, Hengyang Normal University, Hengyang, 421008, Hunan, PR China.
Tel.: +86 734 848 4195.
E-mail address: junhua325@yahoo.com.cn (J. Li).

0304-3894/$ – see front matter © 2011 Elsevier B.V. All rights reserved.
doi:10.1016/j.jhazmat.2011.11.076

alternative to monitor lower concentration of 4-NP in environment. In order to enhance the sensitivity of electrochemical sensors, the working electrode employed in familiar electrochemical technique often needs surface modifying. Recently, Mhammedi et al. [12] used hydroxyapatite modified electrode to investigate the electrochemical behaviors of 4-NP and realize the determination of 4-NP with lower detection limit of 8 nM. Though many other modified electrodes based on carbon nanotubes [13–15], nano-gold [16], silver particles [17] and ionic liquid [18] have been also reported to detect 4-NP with satisfactory results; it is still a challenge to fabricate a new electrochemical sensor based on novel materials with excellent electro-catalysis properties by simpler preparation.

Since the discovery by Geim and co-workers in 2004 [19], graphene, a flat monolayer of sp^2-bonded carbon atoms tightly packed into a two-dimensional honeycomb lattice, and characterized as "the thinnest material in our universe" [19,20], has received considerable attention due to its high surface area ($\sim$2600 m^2/g), high chemical stability, and unique electronic, mechanical properties [21]. This unique nanostructure holds great promise for potential applications in nanoelectronics [22], hybrid [23], lithium ion batteries [24] and sensors [25]. In the past decades, several forms of carbon materials (e.g. C_{60} [23], ordered mesoporous carbon [26], carbon nanofiber [27] and carbon nanotubes [28]) have been used for developing different kinds of electrochemical devices; especially the carbon nanotubes-based electrochemical sensors were most widely investigated. However, several works have demonstrated that graphene usually exhibit better electroanalytical performance than the extensively used carbon nanotubes [29,30]. Graphene oxide (GO), one of the most important derivatives of graphene, also has a large surface area, excellent conductivity and strong mechanical strength. Furthermore, the oxidized rings of functionalized and defective GO sheets contain abundant C—O—C (epoxide) and C—OH groups, while the sheets are terminated with C—OH and —COOH groups [31,32]. Defects of GO may change its electronic and chemical properties. The functionalized and defective GO sheets are more hydrophilic and can be easily dispersed in solvents with long-term stability [33]. Moreover, they are more easily produced in mass quantities as compared with the carbon nanotubes. They may be used to prepare some novel GO-based films, which could facilitate the further manipulation and processing of these materials for developing novel electronic devices, such as chemical sensors and biosensors. Recently, GO-based electrochemical sensors have been developed for the sensitive determination of dopamine [30], caffeine [34], 2,4,6-trinitrotoluene [35] and used as a platform for immobilizing glucose oxidase to construct new glucose biosensors [36].

The aim of this work is to fabricate a novel and stable electrochemical sensor for ultra sensitive determination of 4-NP. The working electrode used in this method was modified with GO which was simply prepared from graphite. Compared with bare electrode, the electro-reduction peak of 4-NP was remarkably heightened at GO modified electrode, and it can be used as an analytical sign for 4-NP determination. The experimental parameters such as the concentration of GO, pH value and accumulation conditions were optimized and the kinetic parameters of the electrode process were detailedly discussed. Finally, this method was successfully applied to determine trace amounts of 4-NP in real water samples with satisfactory results.

2. Experimental

2.1. Reagents

Graphite powder (spectrum pure), H_2SO_4, $KMnO_4$ and H_2O_2 (30 wt%) were obtained from Shanghai Chemical Reagent Co. (China). 4-NP was purchased from Sigma–Aldrich, and its stock solution of 0.01 M was prepared by dissolving the required amount of 4-NP in redistilled water and then kept in darkness at 4 °C. Working solutions were freshly prepared before use by diluting the stock solution. An acetate buffer (pH 4.8) of 0.1 M was always employed as a supporting electrolyte. All other reagents were of analytical reagent grade and used as received. All solutions were prepared with redistilled water, and the solutions were deaerated by bubbling high-purity nitrogen before the experiments. The pH values of the solutions were adjusted with 0.1 M HCl and NaOH.

2.2. Apparatus

All electrochemical experiments were performed on a CHI660D electrochemical workstation (CH Instrumental Co., China) with a conventional three-electrode cell. A bare or modified glassy carbon electrode (GCE, d = 3 mm) was used as working electrode. A saturated calomel electrode (SCE) and a platinum wire were used as reference electrode and auxiliary electrode, respectively. The pH measurements were carried out on PHS-3C exact digital pH meter (Shanghai REX Instrument Factory, China), which was calibrated with standard buffer solution every day. Fourier transform infrared (FTIR) spectra were recorded on a FTIR-8700 infrared sepectrophotometer (Shimadzu, Japan). Scanning electron microscopy (SEM) image was obtained from JSM-6700F field emission SEM system (Jeol, Japan) which was operated at an acceleration voltage of 15.0 kV. Atomic force microscopic (AFM) images were recorded with a Nanoscope IV atomic force microscope (Digital Instruments) using a tapping mode.

2.3. Synthesis of graphene oxide

GO was synthesized directly from graphite by a modified Hummers method [37]. Generally, 1 g graphite was ground with 50 g NaCl for 10 min. NaCl was then dissolved and removed by filtration with water. The remaining graphite was stirred in 23 mL of 98% H_2SO_4 for 8 h. $KMnO_4$ (3 g) was gradually added while keeping the temperature less than 20 °C. The mixture was then stirred at 80 °C for 45 min. Next, the redistilled water of 46 mL was added and the mixture was heated at 105 °C for 30 min. The reaction was terminated by addition of redistilled water (140 mL) and 30% H_2O_2 solution (10 mL). The resulting mixture was washed by repeated centrifugation and filtration, first with 5% HCl aqueous solution and then with distilled water. Finally, the GO product was obtained after dried in vacuum.

2.4. Preparation of modified electrode

For fabrication of modified electrodes, the modifier suspension was prepared by dispersing 10.0 mg GO in 2.5 mL DMF under ultrasonication for 30 min. Prior to modification, a bare GCE was polished to form a mirror-like surface with 0.3 and 0.05 μm alumina slurry on micro-cloth pads, then washed successively with HNO_3—H_2O (1/1 by volume), anhydrous alcohol and redistilled water in an ultrasonic bath and dried in air. Then the prepared suspension of 5.0 μL was coated onto the fresh GCE surface using a micropipette, followed by evaporating the solvent under an infrared lamp. After the solvent was evaporated, the electrode surface was thoroughly rinsed with redistilled water and dried in the air. The obtained electrode was denoted as GO/GCE. In order to eliminate the memory effect, the modified electrode was treated in the blank supporting electrolyte before every measurement by successive cyclic voltammetric sweeps until the steady curve appeared. The modified electrode was stored at 4 °C in a refrigerator when it was not used.

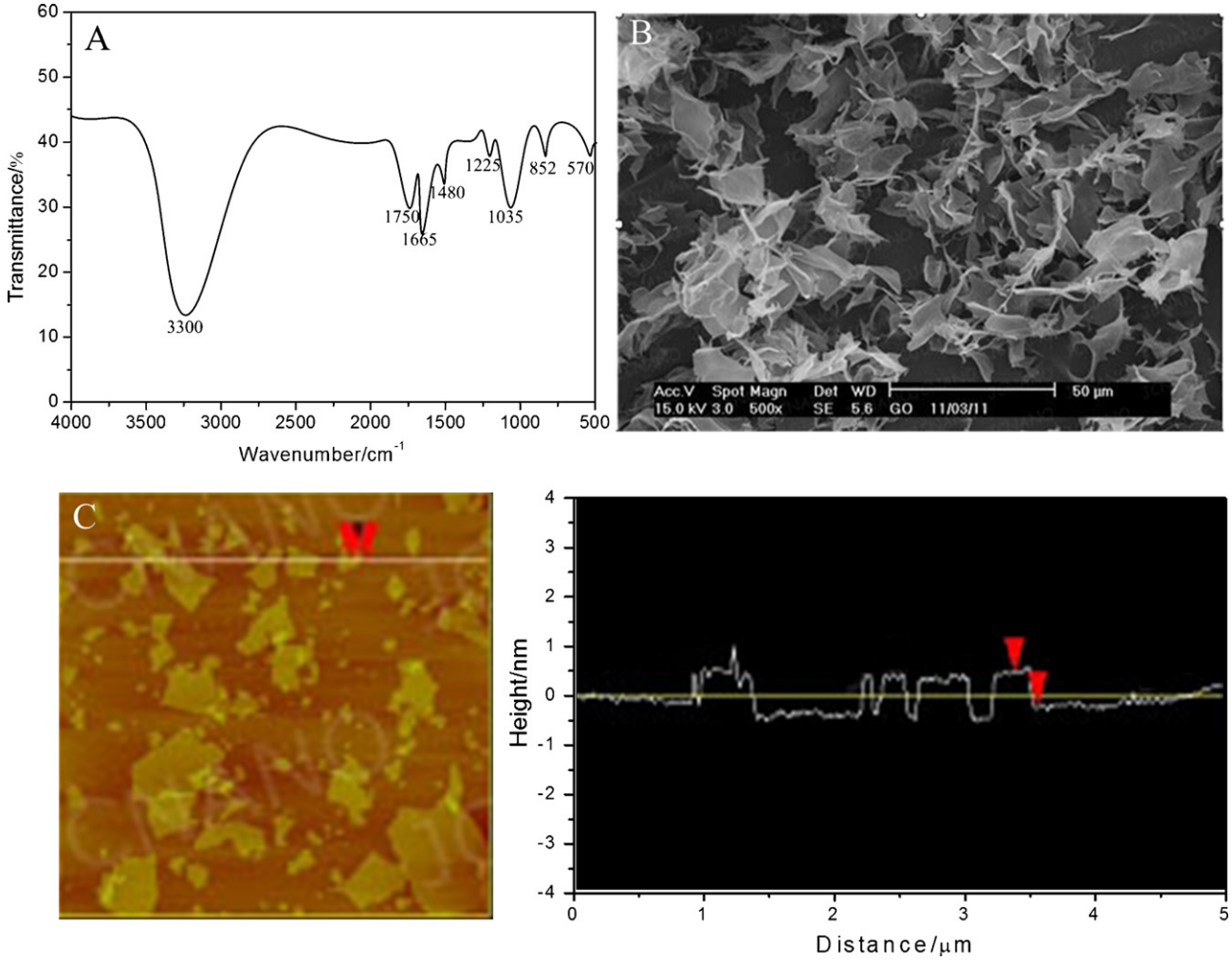

Fig. 1. Characterizations of graphene oxide: (A) FT-IR spectrum of GO, (B) SEM image of GO, (C) AFM image of GO.

3. Results and discussion

3.1. Characterizations of the prepared graphene oxide

The prepared GO was kermesinus and dispersed well in water, DMF and other organic solvent. As shown in Fig. 1A, the spectrum of FT-IR of GO showed that the peak at 3300 cm^{-1} attributes to O—H stretching vibration, the peak at 1750 cm^{-1} attributes to C=O stretching vibration, the peak at 1480 cm^{-1} attributes to deformation of O—H, the peak at 1225 cm^{-1} attributes to vibration of C—O (epoxy), and the peak at 1035 cm^{-1} attributes to vibration of C—O (alkoxy). Then, the Boehm method [38] was further employed to quantify the content of these surface oxygenic functional groups. The total content of oxygen-containing groups was 0.49 mmol/g with 18.4% (0.09 mmol/g) C=O group, 42.9% (0.21 mmol/g) O—H group, and 38.7% (0.19 mmol/g) C—O groups. The experimental results indicated that some functional groups of negative charge were successfully grafted in carbon ring of GO during its preparation. The morphologic characterization of the prepared GO was firstly examined by SEM and the obtained image is shown in Fig. 1B. It can be seen that the basic shapes of the GO look like pieces of the leaves or flakes. It also indicates that GO sheets possess highly porous nanostructure, which may allow the free entry of 4-NP into the inner layers, increasing utilization of the whole film. To further characterize the exact structures of the GO sheets, AFM was employed for getting more information of the internal construction. Fig. 1C shows a tapping-mode AFM image of exfoliated GO sheets. The sample was prepared by depositing a GO aqueous dispersion (0.1 mg mL^{-1}) onto a new cleaved mica surface and dried under vacuum at room temperature. The cross-sectional view of the AFM image indicated that the average thickness of the sheets is about 1.0 nm, which indicated that the GO flakes had single layer. In the image, small GO sheets with a size of 200–300 nm and large sheets with size of more than 1 μm were observed. This unique nanostructure may be attractive as potential material for developing novel types of highly sensitive and stable electrochemical sensors for the determination of 4-NP.

3.2. Electrochemical characterizations of the modified electrode

Electrochemical behaviors of the modified electrode were investigated using $[Fe(CN)_6]^{3-/4-}$ as redox probes by cyclic voltammetry (CV) firstly. Fig. 2A showed the CVs of GCE (a) and GO/GCE (b) recorded in 5 mM $[Fe(CN)_6]^{3-/4-}$ (1:1) solution containing 0.1 M KCl at a scan rate of 100 mV s^{-1}. At bare GCE, a couple of well defined redox peaks were observed with peak-to-peak separation (ΔE_p) of 86 mV. When the electrode was coated with GO, the peak currents of redox peaks decreased obviously, which could be attributed to the negatively charged carboxyl group on GO surface [39,40], blocking the diffusion of $[Fe(CN)_6]^{3-/4-}$ from solution to electrode surface. Moreover, the decrease of ΔE_p (72 mV) was observed at

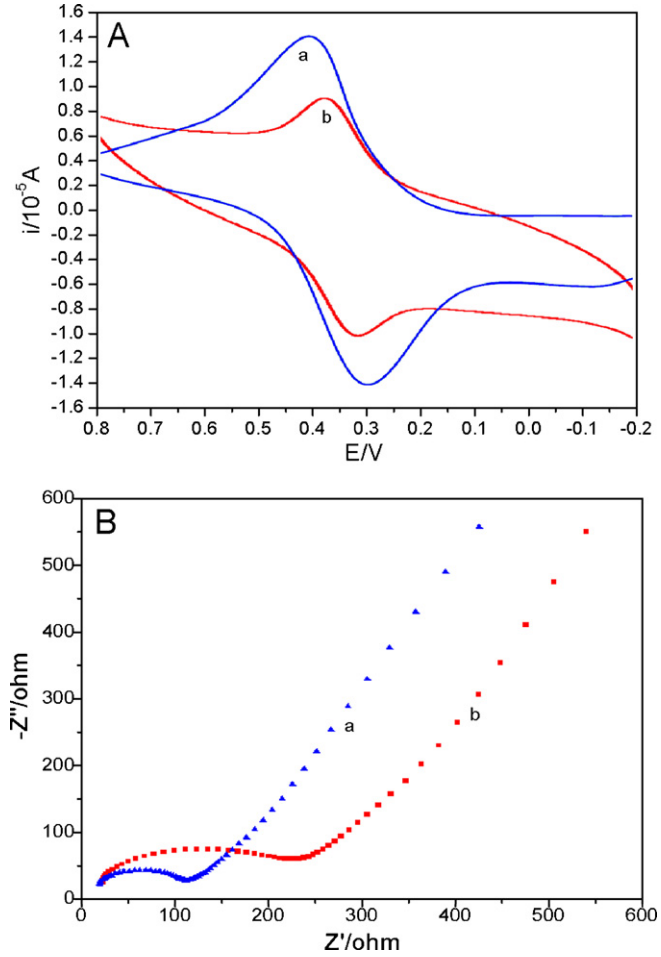

Fig. 2. CVs (A) and EIS (B) of bare GCE (a) and GO/GEC (b) in 5 mM $[Fe(CN)_6]^{3-/4-}$ (1:1) solution containing 0.1 M KCl. The scan rate of CV is 100 mV s^{-1}; the frequency range of EIS was from 0.1 to 10^5 Hz at the formal potential of 0.17 V.

GO/GCE and it indicated that GO film could improve the reversibility of the electrode reaction process.

For further characterization of the modified electrode, the electrochemical impedance spectroscopy (EIS) was used in the frequency range from 0.1 Hz to 10^5 Hz at the different formal potentials (−0.3 to +0.3 V). At the potential of 0.17 V, the Nyquist diagrams formed by semi-circle and straight line curves are most common and representative. So, Fig. 2B presented the Nyquist diagrams of bare GCE (a) and GO/GCE (b) in 5 mM $[Fe(CN)6]^{3-/4-}$ containing 0.1 M KCl at 0.17 V. It can be seen that a small well defined semi-circle at higher frequencies was obtained at the bare GCE, indicated small interface impedance. When GO was deposited on the surface of GCE, the impedance value was much larger than that at GCE, which could be attributed to the negative charges on GO film, introducing a electrostatic repulsion into the electrode/solution system, leading to a lower rate of the electron transfer of $Fe(CN)6^{3-/4-}$. This phenomenon also demonstrated that GO was successfully immobilized on the GCE surface.

3.3. Cyclic voltammetrics of 4-NP

Fig. 3 showed CVs of GCE (a and c) and GO/GCE (b and d) in the absence (a and b) and presence (c and d) of 0.1 mM 4-NP at 100 mV s^{-1}. No redox peak was observed at GCE without 4-NP. The same phenomenon was also obtained at GO/GCE. From this, it can be concluded that GO is electro-inactive in the selected potential

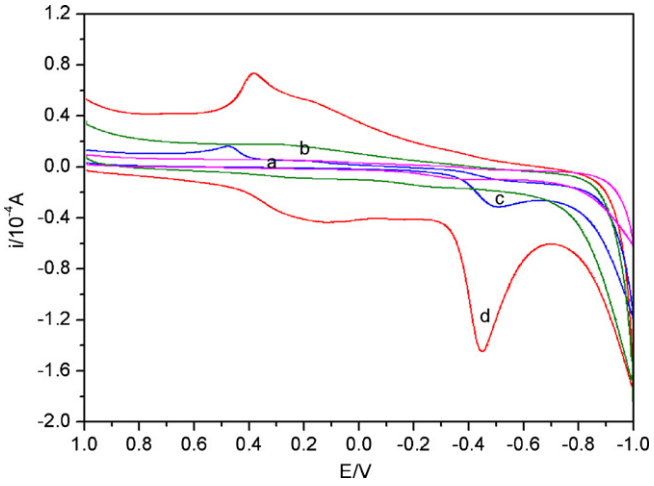

Fig. 3. CVs of GCE (a and c) and GO/GCE (b and d) in the absence (a and b) and presence (c and d) of 0.1 mM 4-NP in 0.1 M acetate buffer. Scan rate: 100 mV s^{-1}; pH: 4.8; accumulation time: 60 s; accumulation potential: 0.2 V.

region. When 0.1 mM 4-NP was added into 10 mL acetate buffer (pH 4.8), 4-NP shows an irreversible behavior at the bare GCE (Fig. 3c) with relatively weak redox current peaks at E_{pa} (anodic peak potential) = 0.475 V and E_{pc} (cathodic peak potential) = −0.502 V. However, as can be seen from Fig. 3d, 4-NP exhibits a pair of well-defined redox waves on the GO/GCE with E_{pa} = 0.382 V and E_{pc} = −0.448 V, and the reduction overpotential of 4-NP becomes lower than that on the bare GCE with a positive shifting of 54 mV. As expected, the redox peak currents are markedly higher than those at the bare GCE, which suggests that GO is an effective mediator in the electrocatalytic redox of 4-NP, and especially the reduction peak current increased larger compared with the oxidation peak current. The obvious enhancement of reduction peak current and positive shift of reduction peak potential indicate that GO exhibits effective catalytic ability to reduce 4-NP, and this is due to the attractive characteristics of GO, such as subtle electronic characteristics and strong adsorptive capability. The GO should have very strong adsorptive capability for 4-NP, because there are several interactions between them. First, the interaction between GO and 4-NP can be hydrogen bonds and some hydrophobic force [37,41], since the —OH and —COOH groups on GO sheet can form strong hydrogen-bonding interaction with —OH and $—NO_2$ groups in 4-NP. Second, 4-NP has an aromatic structure, so there may be π–π stacking between GO and 4-NP. Finally, there may be some electrostatic interaction between GO and 4-NP since there is a nitrogen atom that could be positively charged in 4-NP. These interactions cause the high loading efficiency of 4-NP on GO. Furthermore, the reduced-GO prepared by the chemical reduction of GO with hydrazine [42] exhibited less electro-catalysis effect on redox of 4-NP compared with GO. Because there are few oxygen-containing groups on reduced-GO, its adsorption capacity for 4-NP is lower, resulting in the redox currents of 4-NP on reduced-GO lower than those on GO. In addition, the reduction peak potential obtained at GO/GCE was higher than that at single-wall carbon nanotube coated electrode (−0.72 V, vs. SCE) [13], multi-wall carbon nanotubes-Nafion modified electrode (−1.0 V, vs. SCE) [14] and lithium tetracyanoethylenide modified electrode (−0.70 V, vs. Ag/AgCl) [43] in aid conditions. Therefore, a substantial decrease in reduction overpotential has been achieved in the present study with GO/GCE, and the reduction peak current can be chosen as an analytical signal to detect 4-NP.

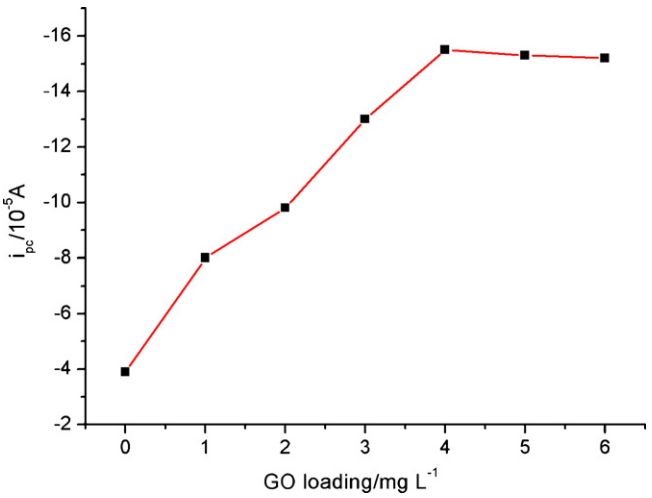

Fig. 4. The effect of GO/DMF concentration on the peak current of 0.1 mM 4-NP. The conditions are the same as those in Fig. 3.

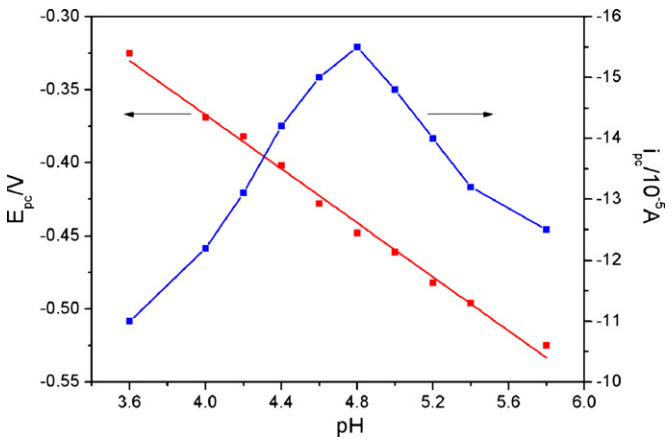

Fig. 5. The effect of pH of buffer solution on the current response and potential response of 0.1 mM 4-NP. Other conditions are the same as those in Fig. 3, except that the pH of buffer solution is variable.

3.4. Optimization of experimental parameters for determination of 4-NP

3.4.1. Effect of GO/DMF concentration

Fig. 4 depicts the influence of concentration of GO/DMF suspension on the reduction peak current of 0.1 mM 4-NP. As gradually improving the content of GO/DMF suspension, the peak current of 4-NP greatly enhances. While increasing the content of GO/DMF suspension from 0 mg mL^{-1} to 4 mg mL^{-1}, the effective surface area and the accumulation efficiency accordingly improve. Consequently, the surface concentration of 4-NP increases and then the reduction peak current also enhances. When further increasing the content from 4 mg mL^{-1} to 6 mg mL^{-1}, the reduction peak current of 4-NP decreases slightly, suggesting that if the modified film is too thick, it is unbeneficial for 4-NP sensing. In this work, the best content of GO/DMF was selected as 4 mg mL^{-1}.

3.4.2. pH effect

The effect of the buffer solution on the sensor response was tested in four different buffer solutions (phosphate, acetate, citrate, and borater) with the concentration of 0.1 M. When the acetate buffer solution was used, the baseline was steady and high sensitivity was obtained. In this sense, the acetate buffer solution was chosen.

The effect of pH on the reduction of 0.1 mM 4-NP at GO/GCE was investigated by CV in the pH range from 3.6 to 5.8. As shown in Fig. 5, the reduction peak current of 4-NP increased gradually with increasing pH from 3.6 to 4.8, and the maximum current was achieved at pH 4.8. With further increasing pH, the reduction peak current conversely decreased. Therefore, pH 4.8 was chosen for the subsequent analytical experiments. With the solution pH increasing from 3.6 to 5.8, the E_{pc} of 4-NP at GO/GCE shifted negatively and linearly. The linear regression equation can be expressed as E_{pc} (mV) = – 0.0923 pH + 0.0022 (R^2 = 0.9931). According to the Nernst equation of $E_{pc} = E^{\theta} - [(2.303mRT)/(nF)]$ pH [44], the ratio of m/n was calculated to be 1.56; where m is the proton number intervening in the reduction process, n is the number of transfer electron, R, T and F have their usual meanings. From this conclusion, it can be known that the proton transfer number could be calculated easily if the number of transfer electron was got.

3.4.3. Scan rate effect

Useful information involving electrochemical mechanism usually can be acquired from the relationship between the peak current and scan rate. The effect of scan rate on the reduction of 4-NP was also investigated. Fig. 6 showed CVs of 0.1 mM 4-NP at GO/GCE with different scan rates. The reduction peak current increased gradually with the increase of scan rate. As shown in the insert of Fig. 6, the reduction peak current increased linearly with the scan rate in the range of 20–250 mV s^{-1} and it can be expressed as: I_{pc} (10^{-4} A) = –4.7033ν (mV s^{-1}) – 87.2051 (R^2 = 0.9852), which indicated that the reduction of 4-NP on GO/GCE is a typical adsorption-controlled process. Consequently, it can be used to preconcentrate micro-quantity of 4-NP onto the surface of GO/GCE for quantitative analysis. In order to decrease the background current and obtain high sensitivity, the scan rate was chosen as 100 mV s^{-1} for the further experiments.

3.4.4. Effect of accumulation conditions

Accumulation can improve the amount of 4-NP absorbed on the electrode surface, and then improve determination sensitivity and decrease detection limit. In order to evaluate the influence of accumulation potential on determination of 4-NP, the reduction peak currents of 0.1 mM 4-NP after 60 s accumulation under different accumulation potentials were measured by linear sweep

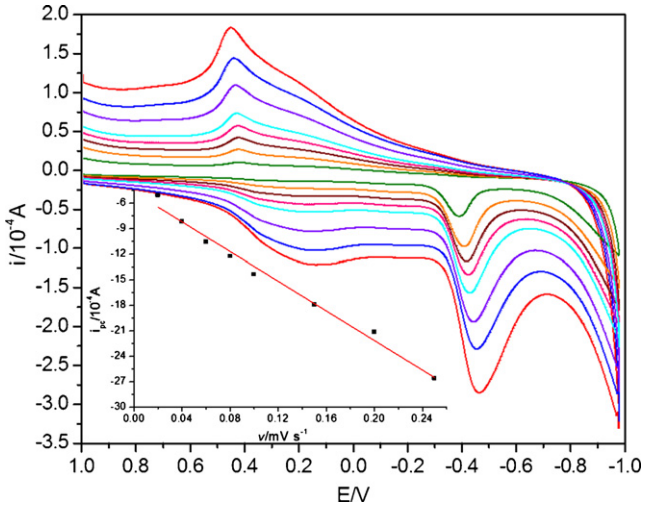

Fig. 6. CVs of 0.1 mM 4-NP at GO/GCE with different scan rates and the plot for the dependence of the reduction peak current on scan rate shown in insert. Curves (inside–outside) are obtained at 20, 40, 60, 80, 100, 150, 200, and 250 mV s^{-1}, respectively. Other conditions are the same as those in Fig. 3, except that the scan rates are variable.

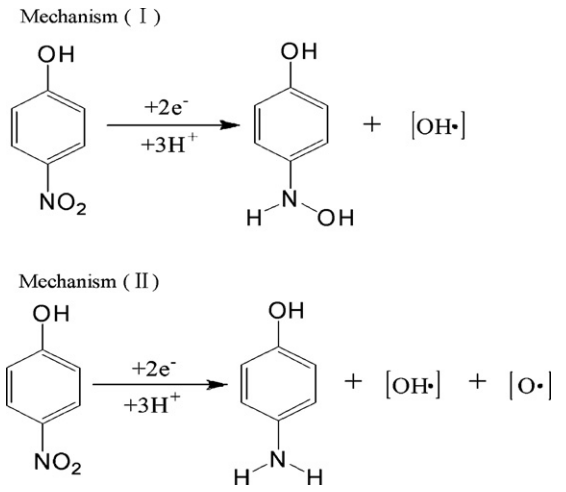

Fig. 7. The possible reduction mechanism of 4-NP at GO/GCE.

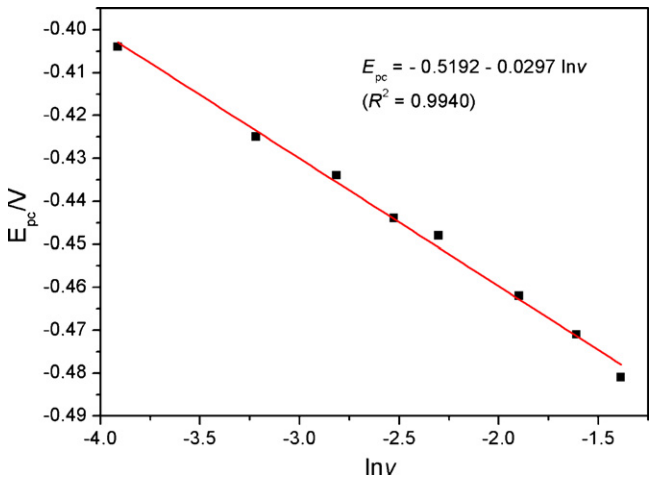

Fig. 8. The plot for the dependence of the reduction peak potential on natural logarithm of scan rate.

voltammetry (LSV). The reduction peak current increased remarkably when the accumulation potential shifted from −0.30 to 0.20 V. However, the downtrend of reduction peak current was obtained under more positive accumulation potential. Therefore, 0.20 V was selected as an optimum accumulation potential for determination of 4-NP. In addition, the reduction peak current increased gradually with accumulation time up to 60 s at a fixed accumulation potential of 0.20 V. More 4-NP could be adsorbed on the electrode surface with extending accumulation time. Afterwards, the peak current increased much slightly as further increasing accumulation time. This phenomenon could be attributed to the saturated adsorption of 4-NP at the electrode surface. Considering both sensitivity and work efficiency, the optimal accumulation time of 60 s was employed in the further experiments.

3.5. Measurement of kinetic parameters of the electrode process

3.5.1. Electron transfer number (n) and proton transfer number (m)

Electron transfer number n is the basic parameter of an electrode reaction. Bulk electrolysis with coulometry was used to determine the electron transfer number of 4-NP reduction process at GO/GCE. The electron transfer number n can be obtained by Frarday equation [45]:

$$n = \frac{\Delta Q}{FcV} \quad (1)$$

where ΔQ is charge involved in the reaction ($\Delta Q = Q_{4\text{-NP}} - Q_{\text{blank}}$), c is concentration of 4-NP, V is volume of electrolyte, F is Faraday constant. From the result of bulk electrolysis with coulometry ($Q_{4\text{-NP}} = 0.2352$ C, $Q_{\text{blank}} = 0.0625$ C, and $c = 0.1$ mM, $V = 10$ mL), the electron transfer number n was calculated to be 2 which is accordant with the previous report [18]. Through the above described, we have got the ratio of $m/n = 1.56$, so the proton transfer number (m) was calculated to be 3. Therefore, the electro-reduction of 4-NP on GO/GCE is a two-electron and three-proton process, and the possible reduction mechanism of 4-NP under our experimental conditions could be deduced in two routes which were listed in Fig. 7. From Fig. 7, it can be seen that the intermediate products of the reduction of 4-NP maybe contain the free radical of OH•, rather than OH^- group. This is because that if the OH^- exists, it can directly produce H_2O as reduction production in acid conditions, but in that case the chemical equation cannot balance. So, we assume that some free radicals of OH• as well as O• may be appear in the electro-reduction process under our experimental conditions.

3.5.2. Charge transfer coefficient (a)

With an increase of scan rate, the cathodic peak potential shifted negatively (seen in Fig. 6). The relationship between E_{pc} and the natural logarithm of scan rate ($\ln \nu$) was shown in Fig. 8. It can be seen that E_{pc} changed linearly vs. $\ln \nu$ with a linear regression equation of E_{pc} (mV) = $-0.5192 - 0.0297 \ln \nu$ ($R^2 = 0.9940$) in the range from 20 to 250 mV s^{-1}. For a totally irreversible electrode process, the relationship between the potential (E_p) and scan rate (ν) could be expressed as following equation given by Laviron [46]:

$$E_p = E^0 + \left(\frac{RT}{\alpha nF}\right) \ln\left(\frac{RTk^0}{\alpha nF}\right) - \left(\frac{RT}{\alpha nF}\right) \ln \nu \quad (2)$$

where a is the electron transfer coefficient, n is the number of transfer electron, R, T and F have their usual meanings. Thus, the value of αn can be easily calculated from the slope of E_{pc} vs. $\ln \nu$. In this system, the value of αn was calculated to be 0.86 (taking $T = 298$, $R = 8.314$, and $F = 96\,500$). According to foregoing research results, as $n = 2$, α can be calculated to be 0.43.

3.5.3. Effective surface area (A) and diffusion coefficient (D)

The electrochemical effective surface area for bare GCE and GO/GCE can be calculated by the slope of the plot of Q vs. $t^{1/2}$ obtained by chronocoulometry using 0.5 mM $K_3[Fe(CN)_6]$ as model complex based on the equation (3) given by Anson [47]:

$$Q(t) = \frac{2nFAcD^{1/2}t^{1/2}}{\pi^{1/2}} + Q_{\text{dl}} + Q_{\text{ads}} \quad (3)$$

where A is effective surface area of working electrode, c is concentration of substrate, n is the number of transfer electron (n of $K_3[Fe(CN)_6]$ is 1), D is diffusion coefficient (D of $K_3[Fe(CN)_6]$ is 7.6×10^{-6} cm^2 s^{-1} [48]), Q_{dl} is double layer charge which could be eliminated by background subtraction, Q_{ads} is Faradaic charge. Other symbols have their usual meanings. Based on the slope of the linear relationship between Q and $t^{1/2}$ in Fig. 9, the effective surface area A could be calculated to be 0.0791 cm^2 and 0.1735 cm^2 for GCE and GO/GCE, respectively. The results indicated that the electrode effective surface area was increased obviously after electrode modification, which would increase the adsorption capacity of 4-NP, leading to enhance current response for the prepared electrochemical sensor. The diffusion coefficient (D) and Faradic charge (Q_{ads}) of 4-NP at GO/GCE can also be measured using chronocoulometry based on Eq. (3). After background subtraction, the plot of Q against $t^{1/2}$ showed a linear relationship with slope of 3.569×10^{-4} $C/s^{1/2}$ and Q_{ads} of 3.1827×10^{-5} C. As $n = 2$, $A = 0.1735$ cm^2 and $c = 0.1$ mM,

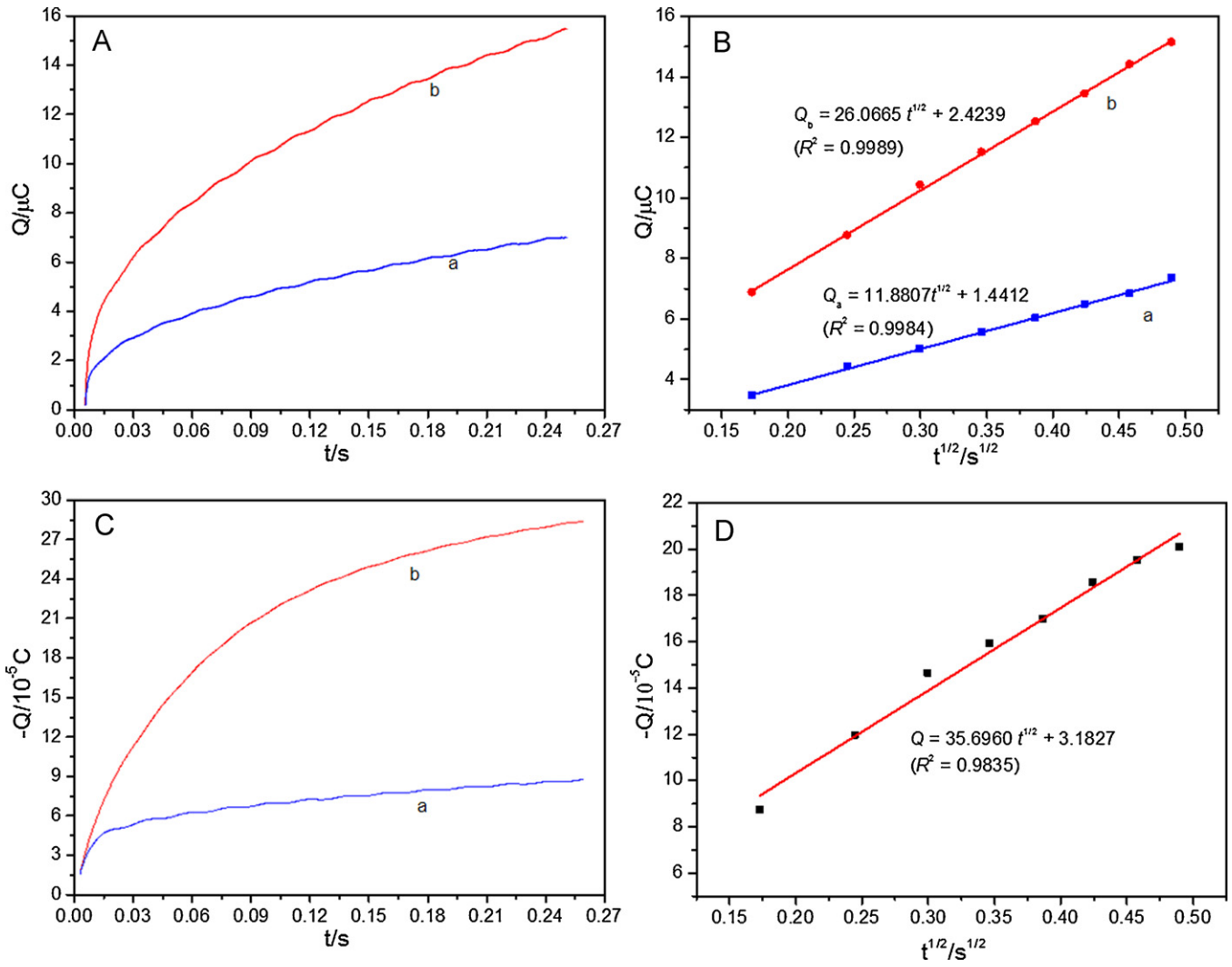

Fig. 9. (A): Plot of Q–t curves for the GCE (a) and GO/GCE (b) in 0.5 mM $K_3[Fe(CN)_6]$; (B): plot of Q–$t^{1/2}$ curves for the GCE (a) and GO/GCE in 0.5 mM $K_3[Fe(CN)_6]$; (C): Plot of Q–t curves for GO/GCE in 0.1 M acetate buffer (pH 4.8) in absence of (a) and in present of (b) 0.1 mM 4-NP; (D): plot of Q–$t^{1/2}$ curve for GO/GCE in present of 0.1 mM 4-NP (background subtracted).

D was calculated to be 8.896×10^{-5} cm^2 s^{-1}. According to the equation of $Q_{ads} = nFA\Gamma_s$, the adsorption capacity of Γ_s could be obtained as 9.505×10^{-8} mol cm^{-2} which is much higher than that at ionic liquid modified electrode (2.47×10^{-9} mol cm^{-2}) [18] and hydroxyapatite modified electrode (7.12×10^{-10} mol cm^{-2}) [5]; and the obtained Γ_s is also higher than the coverage of monomolecular layer, so it further demonstrates that GO has excellent adsorption property toward 4-NP.

3.5.4. Standard heterogeneous rate constant (k_s)

The standard heterogeneous rate constant (k_s) for totally irreversible reduction of 4-NP at the modified electrode was calculated based on Eq. (4) [49]:

$$k_s = 2.415 \exp\left(\frac{-0.02F}{RT}\right) D^{1/2}(E_p - E_{p/2})^{-1/2}V^{1/2} \quad (4)$$

where E_p and $E_{p/2}$ represent the peak potential and the half-height potential in LSV, respectively. Other symbols have their usual meanings. In this work, $E_p - E_{p/2} = 101$ mV, $D = 8.896 \times 10^{-5}$ cm^2 s^{-1}, $v = 100$ mV s^{-1}, and $T = 298$ K. Therefore, k_s was calculated to be 1.544×10^{-3} cm s^{-1}.

3.6. Calibration curve

In order to obtain an analytical curve for the fabricated sensor, the quantitative analysis of 4-NP concentration using GO/GCE was performed with LSV under the optimized experimental conditions and the results were shown in Fig. 10. It can be seen that the cathodic peak current was proportional to 4-NP concentration in the range of 0.1–120 μM. The linear regression equation can be expressed as I_{pc} (10^{-5} A) = −3.5094 C (10^{-9} M) − 0.1075, with a correlation coefficient of 0.9975. The linear range was broader than the reported ranges obtained from some modified electrodes such as silver amalgam paste electrode [2], apatite/CPE [12], MWNT-Nafion/GCE [14] and silver particles/GCE [17]. The detection limit (S/N = 3) is estimated to be 0.02 μM, lower than those from hydroxyapatite-based [5], MWNT-based [15] and gold-based [16] electrochemical sensors. The lower detection limit indicated that the proposed method could potentially be used to sensitively monitor 4-NP concentration. A detailed comparison of the performances of different electrochemical sensors for the determination of 4-NP is summarized in Table 1. From Table 1, it can be concluded that the GO/GCE is an excellent platform for the detection of 4-NP, and the superior performance of the prepared sensor could be

Table 1
Comparison of the performances of different electrochemical sensors for 4-NP.

Electrode materials	Linear range (μM)	Correlation coefficient	Detection limit (μM)	Stability keep	Recovery (%)	References
AgA-PE[a]	0.2–100	–	0.3	–	–	[2]
HN[b]/GCE[c]	1.0–300	0.9996	0.6	82% (30 days)	96–104	[5]
Apatite/CPE	0.2–100	0.9835	0.008	–	86.2	[12]
SWNT[d]/GCE	0.01–5	–	0.0025	93.5% (14 days)	98.8–104.2	[13]
MWNT[e]-Nafion/GCE	0.1–10	0.9980	0.04	94.4% (12 h)	102.6–104.6	[14]
MWNT/GCE	2–4000	0.9965	0.4	–	96–102	[15]
Nano-gold/GCE	10–1000	–	8	95% (7 days)	97–97.7	[16]
Silver particles/GCE	1.5–140	0.9800	0.5	–	–	[17]
Ionic liquid/CPE[f]	3–800	0.9940	0.1	–	–	[18]
LiTCNE[g]/GCE	0.027–23.2	0.9990	0.0075	–	101.1–105	[43]
SMA[h]/GCE	0.3–45 mg L^{-1}	0.9976	0.02 mg L^{-1}	–	99.5–102.2	[50]
Nanoporous gold	0.5–10 mg L^{-1}	0.9941	–	–	–	[51]
Nano-Cu_2O/Pt electrode	10–1000	0.9985	0.1	–	–	[52]
GO/GCE	0.1–120	0.9975	0.02	83% (30 days)	99.0–102.3	This work

[a] AgA-PE: silver amalgam paste electrode.
[b] HN: hydroxyapatite nanopowder.
[c] GCE: glassy carbon electrode.
[d] SWNT: single-wall carbon nanotubes.
[e] MWNT: multi-wall carbon nanotubes.
[f] CPE: carbon paste electrode.
[g] LiTCNE: lithium tetracyanoethylenide.
[h] SMA: sodium montmorillonite–anthraquinone.

ascribed to the electrocatalytic activity and the adsorption ability of GO.

3.7. Reproducibility, stability and interference

The fabrication reproducibility for ten modified electrodes was carried out by comparing the reduction peak current of 0.1 mM 4-NP. The relative standard deviation (RSD) was 3.25%, revealing that this method had good reproducibility. The stability of the electrode was also investigated by measuring the electrode response with 0.1 mM 4-NP every 10 days. Between measurements the electrode was stored at 4 °C in a refrigerator. The current response decreased to 90% after 10 days, while 86% of the original response retained after 20 days. The electrode still retained 83% of its original response even after 30 days.

On the other hand, in order to evaluate the selectivity of the prepared sensor, the influence of some possible interfering substances was examined in pH 4.8 acetate buffer containing 4-NP of 0.1 mM and 0.1 μM, respectively (shown in Table 2). It can be seen that most of the phenols had no influence on the signals of 4-NP with deviations below 5%, but the nitrophenols were found to affect the determination because they contain the same nitro groups that can be reduced near the potential of 4-NP. However, their influence is not significant at low concentrations. Additionally, some inorganic ions such as 500-fold concentration of Na^+, K^+, Mg^{2+}, Ca^{2+}, Ni^{2+}, Co^{2+}, Cu^{2+}, Cl^-, Br^-, I^-, NO_3^-, SO_4^{2-}, have no influence on the signals of 4-NP with deviations below 3%. The results obtained from reproducibility, stability and interference tests indicated that GO/GCE might be suitable for analytical application.

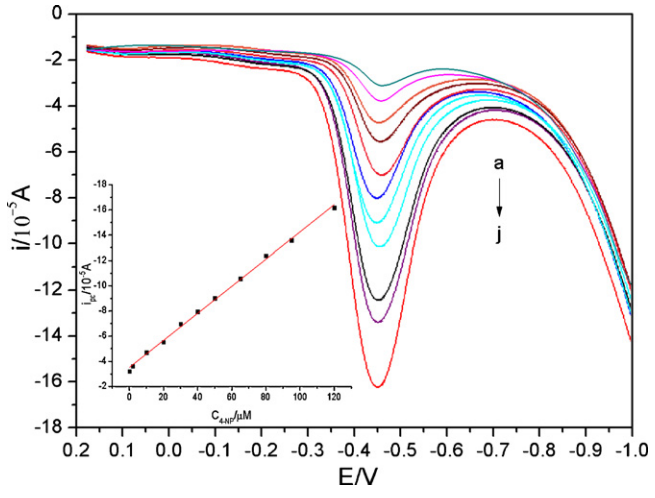

Fig. 10. LSV responses of increasing 4-NP concentration, from a to j, 0.1, 2, 10, 20, 30, 40, 50, 65, 80, 95, 120 μM, respectively. Insert: the dependence of peak currents on the concentrations of 4-NP. The other conditions are the same as those in Fig. 3.

3.8. Analytical application

The possibility of applying the present electrochemical method for 4-NP determination in five real water samples from the locality was evaluated. No signals for 4-NP were observed when these water samples were analyzed, which may be attributed to that no 4-NP is in water samples or the concentration of 4-NP is lower than the detection limit. Thus, the determination of 4-NP concentration was performed by the standard addition method. The results are listed in Table 3. It can be seen that the results of proposed method are in agreement with the value obtained by HPLC method [53]. However, HPLC method needs more cost for reagent, on the contrary electrochemical method has many advantages such as low cost, easy fabrication and simple operation, so it is worthy of

Table 2
Influence of interferences on the determination of 4-NP ($n = 3$).

Interfering substances	Concentration (mM)[a]	Relative error (%)	Concentration (μM)[b]	Relative error (%)
Phenol	10	0.36	1	0.12
Pyrocatechol	10	−2.12	1	1.34
Hydroquinone	10	3.53	1	−2.33
Hydroxyphenol	10	3.12	1	−1.15
Phloroglucinol	10	−1.35	1	1.26
2-Aminophenol	10	0.63	1	0.45
4-Aminophenol	10	−1.02	1	−0.69
2-Chlorophenol	10	1.53	1	1.59
4-Chlorophenol	10	1.24	1	−1.62
Bisphenol A	10	4.03	1	3.81
2-Nitrophenol	1	15.32	0.1	5.35
3-Nitrophenol	1	12.71	0.1	5.27
2,4-Dinitrophenol	1	10.89	0.1	4.88

[a] Coexisting 4-NP of 0.1 mM.
[b] Coexisting 4-NP of 0.1 μM.

Table 3
Determination of 4-NP in water samples by GO/GCE.

Samples	Added (μM)	Found[a] (μM)		Relative error (%)	RSD[b] (%)	Recovery (%)
		HPLC method	Proposed method			
Drinking water	5.0	4.83	4.95	2.48	3.25	99.0
Lake water	10.0	9.77	9.92	1.54	3.14	99.2
River water	15.0	15.29	15.34	0.33	2.66	102.3
Underground water	20.0	20.26	20.04	−1.09	4.12	100.2
Domestic sewage	25.0	25.45	25.28	−0.67	3.87	101.1

[a] Average value of five measurements.
[b] Relative standard deviation for the proposed method ($n = 5$).

development. It is also clear that the recoveries of the developed method are in the range from 99.0% to 102.3%. These results indicate that the proposed method should be reliable, effective and sufficient for 4-NP determination. Additionally, the interferences in water samples can be almost neglected.

4. Conclusion

A novel GO-based electrochemical sensor for 4-NP was successfully fabricated and the performance of this sensor was dramatically improved due to the excellent electrical conductivity, strong adsorptive ability and large effective surface area of GO. The modified electrode exhibited a high electrocatalytic activity and good selectivity toward the reduction of 4-NP. Compared with the bare electrode, the reduction current of 4-NP increased greatly and the reduction peak potential shifted positively, and the fabricated sensor was applied to detect 4-NP in water samples with satisfied recoveries from 99.0% to 102.3%. These results indicated that GO was a good candidate of advanced electrode materials and could be combined with other functional materials to fabricate the sensing interface for more applications in the fields of electroanalysis.

Acknowledgements

This work is kindly supported by the supports of the Open Fund Project of Key Laboratory in Hunan Universities (nos. 09K099, 10K010) and the Youth Backbone Teacher Training Program of Hengyang Normal University (2010).

References

[1] P. Mulchandani, C.M. Hangarter, Y. Lei, W. Chen, A. Mulchandani, Amperometric microbial biosensor for p-nitrophenol using moraxella sp.-modified carbon paste electrode, Biosens. Bioelectron. 21 (2005) 523–527.
[2] A. Niaz, J. Fischer, J. Barek, B. Yosypchuk, Sirajuddin, M.I. Bhanger, Voltammetric determination of 4-nitrophenol using a novel type of silver amalgam paste electrode, Electroanalysis 21 (2009) 1786–1791.
[3] E. Lypczynska-Kochany, Degradation of aqueous nitrophenols and nitrobenzene by means of the Fenton reaction, Chemosphere 22 (1991) 529–536.
[4] X. Guo, Z. Wang, S. Zhou, The separation and determination of nitrophenol isomers by high-performance capillary zone electrophoresis, Talanta 64 (2004) 135–139.
[5] H. Yin, Y. Zhou, S. Ai, X. Liu, L. Zhu, L. Lu, Electrochemical oxidative determination of 4-nitrophenol based on a glassy carbon electrode modified with a hydroxyapatite nanopowder, Microchim. Acta 169 (2010) 87–92.
[6] M. Castillo, R. Domingues, M.F. Alpendurada, D. Barcelo, Persistence of selected pesticides and their phenolic transformation products in natural waters using off-line liquid solid extraction followed by liquid chromatographic techniques, Anal. Chim. Acta 353 (1997) 133–142.
[7] A. Niazi, A. Yazdanipour, Spectrophotometric simultaneous determination of nitrophenol isomers by orthogonal signal correction and partial least squares, J. Hazard. Mater. 146 (2007) 421–427.
[8] W. Zhang, C.R. Wilson, Indirect fluorescent determination of selected nitro-aromatic and pharmaceutical compounds via UV-photolysis of 2-phenylbenzimidazole-5-sulfonate, Talanta 74 (2008) 1400–1407.
[9] J.A. Padilla-Sánchez, P. Plaza-Bolaños, R. Romero-González, A. Garrido-Frenich, J.L.M. Vidal, Application of a quick, easy, cheap, effective, rugged and safe-based method for the simultaneous extraction of chlorophenols, alkylphenols, nitrophenols and cresols in agricultural soils, analyzed by using gas chromatography-triple quadrupole-mass spectrometry/mass spectrometry, J. Chromatogr. A 1217 (2010) 5724–5731.
[10] D. Hofmann, F. Hartmann, H. Herrmann, Analysis of nitrophenols in cloud water with a miniaturized light-phase rotary perforator and HPLC–MS, Anal. Bioanal. Chem. 391 (2008) 161–169.
[11] H. Lund, O. Hammerich, Organic Electrochemistry, 4th ed., Marcel Dekker, New York, 2001.
[12] M.A.E. Mhammedi, M. Achak, M. Bakasse, A. Chtaini, Electrochemical determination of para-nitrophenol at apatite-modified carbon paste electrode: application in river water samples, J. Hazard. Mater. 163 (2009) 323–328.
[13] C. Yang, Electrochemical determination of 4-nitrophenol using a single-wall carbon nanotube film-coated glassy carbon electrode, Microchim. Acta 148 (2004) 87–92.
[14] W. Huang, C. Yang, S. Zhang, Simultaneous determination of 2-nitrophenol and 4-nitrophenol based on the multi-wall carbon nanotubes Nafion-modified electrode, Anal. Bioanal. Chem. 375 (2003) 703–707.
[15] L.Q. Luo, X.L. Zou, Y.P. Ding, Q.S. Wu, Derivative voltammetric direct simultaneous determination of nitrophenol isomers at a carbon nanotube modified electrode, Sens. Actuators B 135 (2008) 61–65.
[16] L. Chu, L. Han, X. Zhang, Electrochemical simultaneous determination of nitrophenol isomers at nano-gold modified glassy carbon electrode, J. Appl. Electrochem. 41 (2011) 687–694.
[17] I.G. Casella, M. Contursi, The electrochemical reduction of nitrophenols on silver globular particles electrodeposited under pulsed potential conditions, J. Electrochem. Soc. 154 (2007) 697–702.
[18] W. Sun, M.X. Yang, Q. Jiang, K. Jiao, Direct electrocatalytic reduction of p-nitrophenol at room temperature ionic liquid modified electrode, Chin. Chem. Lett. 19 (2008) 1156–1158.
[19] K.S. Novoselov, A.K. Geim, S.V. Morozov, D. Jiang, Y. Zhang, S.V. Dubonos, I.V. Grigorieva, A.A. Firsov, Electric field effect in atomically thin carbon films, Science 306 (2004) 666–669.
[20] A.K. Geim, K.S.Novoselov, The rise of grapheme, Nat. Mater. 6 (2007) 183–191.
[21] D.A. Dikin, S. Stankovich, E.J. Zimney, R.D. Piner, G.H.B. Dommett, G. Evmenenko, S.T. Nguyen, R.S. Ruoff, Preparation and characterization of graphene oxide paper, Nature 448 (2007) 457–460.
[22] R.M. Westervelt, Applied physics: graphene nanoelectronics, Science 320 (2008) 324–325.
[23] X. Zhang, Y. Huang, Y. Wang, Y. Ma, Z. Liu, Y. Chen, Synthesis and characterization of a graphene–C_{60} hybrid material, Carbon 47 (2009) 334–337.
[24] H. Wang, L.F. Cui, Y. Yang, H.S. Casalongue, J.T. Robinson, Y. Liang, Y. Cui, H. Dai, Mn_3O_4-graphene hybrid as a high-capacity anode material for lithium ion batteries, J. Am. Chem. Soc. 132 (2010) 13978–13980.
[25] J. Zhao, G. Chen, L. Zhu, G. Li, Graphene quantum dots-based platform for the fabrication of electrochemical biosensors, Electrochem. Commun. 13 (2011) 31–33.
[26] C. You, X. Xu, B. Tian, J. Kong, D. Zhao, B. Liu, Electrochemistry and biosensing of glucose oxidase based on mesoporous carbons with different spatially ordered dimensions, Talanta 78 (2009) 705–710.
[27] X. Tang, Y. Liu, H. Hou, T. You, A nonenzymatic sensor for xanthine based on electrospun carbon nanofibers modified electrode, Talanta 83 (2011) 1410–1414.
[28] B. Rezaei, S. Damiri, Using of multi-walled carbon nanotubes electrode for adsorptive stripping voltammetric determination of ultratrace levels of RDX explosive in the environmental samples, J. Hazard. Mater. 183 (2010) 138–144.
[29] H. Yin, Y. Zhou, Q. Ma, T. Liu, S. Ai, L. Zhu, Electrochemical oxidation behavior of guanosine-5(-monophosphate on a glassy carbon electrode modified with a composite film of graphene and multi-walled carbon nanotubes, and its amperometric determination, Microchim. Acta 172 (2011) 343–349.
[30] Y. Wang, Y. Li, L. Tang, J. Lu, J. Li, Application of graphene-modified electrode for selective detection of dopamine, Electrochem. Commun. 11 (2009) 889–892.
[31] K. Nakada, M. Fujita, G. Dresselhaus, Edge state in graphene ribbons: nanometer size effect and edge shape dependence, Phys. Rev. B. 54 (1996) 17954–17961.
[32] H. He, J. Klinowski, M. Forster, A new structure model for graphite oxide, Chem. Phys. Lett. 287 (1998) 53–56.
[33] S. Stankovich, R.D. Piner, X. Chen, N. Wu, S.T. Nguyen, R.S. Ruoff, Stable aqueous dispersions of graphitic nanoplatelets via the reduction of exfoliated graphite oxide in the presence of poly(sodium 4-styrenesulfonate), J. Mater. Chem. 16 (2006) 155–158.
[34] J.Y. Sun, K.J. Huang, S.Y. Wei, Z.W. Wu, F.P. Ren, A graphene-based electrochemical sensor for sensitive determination of caffeine, Colloid Surf. B 84 (2011) 421–426.

[35] M.S. Goh, M. Pumera, Graphene-based electrochemical sensor for detection of 2,4,6-trinitrotoluene (TNT) in seawater: the comparison of single-, few-, and multilayer graphene nanoribbons and graphite microparticles, Anal. Bioanal. Chem. 399 (2011) 127–131.
[36] Y. Zhang, X. Sun, L. Zhu, H. Shen, N. Jia, Electrochemical sensing based on graphene oxide/Prussian blue hybrid film modified electrode, Electrochim. Acta 56 (2011) 1239–1245.
[37] W.S. Hummers, R.E. Offeman, Preparation of graphitic oxide, J. Am. Chem. Soc. 80 (1958) 1339.
[38] H.P. Boehm, Some aspects of the surface chemistry of carbon blacks and other carbons, Carbon 32 (1994) 759–769.
[39] X. Song, Y. Yang, J. Liu, H. Zhao, PS colloidal particles stabilized by graphene oxide, Langmuir 27 (2011) 1186–1191.
[40] Y. Bao, J. Song, Y. Mao, D. Han, F. Yang, L. Niu, A. Ivaska, Graphene oxide-templated polyaniline microsheets toward simultaneous electrochemical determination of AA/DA/UA, Electroanalysis 23 (2011) 878–884.
[41] M. Hirata, T. Gotou, S. Horiuchi, M. Fujiwara, M. Ohba, Thin-film particles of graphite oxide 1: high-yield synthesis and flexibility of the particles, Carbon 42 (2004) 2929–2937.
[42] D. Li, M.B. Müller, S. Gilje, R.B. Kaner, G.G. Wallace, Processable aqueous dispersions of graphene nanosheets, Nat. Nanotechnol. 3 (2008) 101–105.
[43] R.C.S. Luz, F.S. Damos, A.B. Oliveira, J. Beck, L.T. Kubota, Voltammetric determination of 4-nitrophenol at a lithium tetracyanoethylenide (LiTCNE) modified glassy carbon electrode, Talanta 64 (2004) 935–942.
[44] C. Zhou, Z. Liu, Y. Dong, D. Li, Electrochemical behavior of o-nitrophenol at hexagonal mesoporous silica modified carbon paste electrodes, Electroanalysis 21 (2009) 853–858.
[45] C.A. Ma, Introduction to Synthetic Organic Electrochemistry, Science Press, Beijing, 2002.
[46] E. Laviron, General expression of the linear potential sweep voltammogram in the case of diffusionless electrochemical systems, J. Electroanal. Chem. 101 (1979) 19–28.
[47] F. Anson, Application of potentiostatic current integration to the study of the adsorption of cobalt (III)-(ethylenedinitrilo (tetraacetate)) on mercury electrodes, Anal. Chem. 36 (1964) 932–934.
[48] R. Adams, Electrochemistry at Solid Electrodes, New York, M. Dekker, 1969.
[49] J. Velasco, Determination of standard rate constants for electrochemical irreversible processes from linear sweep voltammograms, Electroanalysis 9 (1997) 880–882.
[50] S. Hu, C. Xu, G. Wang, D. Cui, Voltammetric determination of 4-nitrophenol at a sodium montmorillonite–anthraquinone chemically modified glassy carbon electrode, Talanta 54 (2001) 115–123.
[51] Z. Liu, J. Du, C. Qiu, L. Huang, H. Ma, D. Shen, Y. Ding, Electrochemical sensor for detection of p-nitrophenol based on nanoporous gold, Electrochem. Commun. 11 (2009) 1365–1368.
[52] Y. Gu, Y. Zhang, F. Zhang, J. Wei, C. Wang, Y. Du, W. Ye, Investigation of photoelectrocatalytic activity of Cu_2O nanoparticles for p-nitrophenol using rotating ring-disk electrode and application for electrocatalytic determination, Electrochim. Acta 56 (2010) 953–958.
[53] J.H. Li, G.R. Li, H.B. Tang, X.Y. Xu, Y.F. Ouyang, Y.S. Wang, H.M. Yang, Determination of α-naphthol, ß-naphthol, p-nitrophenol and m-nitrophenol in human urine by reversed phase high performance liquid chromatography, Chin. J. Spectrosc. Lab. 28 (2011) 782–786.